# A 2.5 MHz 2D Array with Z-Axis Electrically Conductive Backing

M. Greenstein, P. Lum, H. Yoshida, M.S. Seyed-Bolorforosh*
Hewlett-Packard Laboratories, P.O. Box 10350, Palo Alto, CA 94303
* Currently at General Electric Medical Systems, P.O. Box 414, Milwaukee, WI 53201

*Abstract*

The design, fabrication and initial testing of a prototype fully l/2 sampled, 2500 element 2D phased array is presented. The array utilizes a unique Z-axis electrical conductivity backing layer, to provide both acoustic attenuation and electrical interconnect for the signal channels. The electrical interconnect is designed to be in the acoustic shadow of the transducer elements so as to minimize the foot print of the array. A modular, demountable Pad Grid Array inter connect is used to connect to the backing of the array. Results are presented for measurements of the single element properties of electrical impedance, pulse echo waveform and spectrum, directivity and cross talk.?

## I. Introduction

There has been much discussion in the recent literature about the need and desirability of 2D acoustic phased arrays for medical imaging. Most of the work discussed has been simulations of the arrays because of the difficulty in actually building such arrays. The theoretical aspects of 2D arrays have been discussed [1], [2]. There has also been discussion about the use of 2D arrays to enable 3D ultrasound imaging [3], and phase aberration correction [4]. Extensive experimental work has been done on coarsely sampled 2D arrays [5], [6], as well as multilayer approaches to 2D arrays [7]. Additional theoretical work has been done on the design and the performance of sparse 2D arrays [8] in an attempt to reduce the number of elements, and thus the required number signal channels.

There has not been extensive discussion on the fabrication of fully sampled, λ/2 pitch 2D phased arrays. Such arrays are difficult to build and the number of potential signal channels exceeds the capability of most present day commercial medical ultrasound machines. The interconnection of such densely sampled arrays is also a substantial challenge. This paper discusses the design, fabrication and initial single element characterization of a fully λ/2 sampled 2D phased array, and the demountable interconnect system used with this array.



## II. Array Design and Fabrication

### A. Design

The present 2D array was designed with the following objectives. The design center frequency was chosen to be 2.5 MHz, motivated by the penetration depth for cardiac applications, the obtainable spatial resolution, and the relative ease of fabrication. An active aperture of 15 mm was chosen to match the typical acoustic window between the ribs for transthoracic ultrasound measurements. The array was sampled at λ/2 in order to provide full capability for steering and focussing, resulting in a 50 x 50 array with 2500 active elements. A Z-axis electrically conductive backing layer was developed in order to allow for the electrical interconnect to come through the backing layer, in the acoustic shadow of the elements, and mate to a modular and demountable interconnect system. This approach allows the array to be tested as a separate module before committing it to the interconnect.

The array was designed with a PZT piezoelectric layer with inactive oversized guard elements surrounding the active elements. These inactive guard elements, at the periphery of the array, protect the interior active elements from physical damage. The transducer elements were diced to provide acoustic isolation and then back filled with an epoxy and glass microsphere mixture to increase the mechanical robustness of the individual elements. In Figure 1 a partial top view of the array is shown, drawn to scale. At the upper left corner is a large square inactive guard element, shown hatched. The top row and the left column are also peripheral inactive guard elements. The active elements are shown with a small black square in the middle of each element. This black square represents the cross sectional end of the Z-axis electrical conductor in the backing. The active elements are 250 x 250 μm in cross section.

For the piezoelectric layer, PZT-5H [9] was chosen for its acoustic properties and for its machinability. The matching layer was fabricated from epoxy impregnated graphite [10]. The backing layer was chosen for its acoustic properties and for its Z-axis electrical conductivity. The acoustic properties of the backing layer were determined by an electrically insulating epoxy matrix with Tungsten powder to increase the attenua-

tion [11]. The electrical conductivity properties were determined by imbedded BeCu wires, discussed below.

### *B. Fabrication*

The concept of electrically conductive paths in an otherwise electrically insulating backing material is not new. A general concept for 1D and 2D arrays has been discussed in the patent literature [12]. The use of etched BeCu leadframe material in an otherwise insulating matrix provides the desired electrical conductivity from the rear electrode of the piezoelectric resonator to the rear of the backing layer, and a manageable and scalable approach to imbed such conductive paths in the insulating matrix material. Two leadframes are required for each column of the array. One is the trace leadframe for the desired electrical conductivity path, and the other is the spacer leadframe to ensure the correct spatial pitch of the traces. A typical pair of leadframes is shown schematically in Figure 2. The window frame area at the periphery of each leadframe is used for support and alignment, and is eventually trimmed and discarded. The trace leadframe is 50 μm thick and 50 μm wide at the piezoelectric element. It flares to 100 μm wide at the rear of the backing layer to increase the contact area with the interconnect system discussed in Section III. This flaring is not shown in Figure 2 for simplicity. At the rear of the piezoelectric element a 50 x 50 μm stub of BeCu, which is 4% of the transducer element area, has no measurable effect on the impulse response of the 250 x 250 μm size acoustic element.

The leadframes are etched from BeCu sheets and are plated with CrAu for passivation against corrosion. The leadframes are then stacked into a fixture where they are aligned, stretched and potted into the insulating acoustic backing material. The backing is cured for 24 hours at 70 C. In Figure 3 a side cross sectional view is shown of the potted leadframe structure. The hatched areas are the spacer leadframes and the solid areas are the trace leadframes. The dotted line represents final machined dimensions for the backing layer. Such a Z-axis electrically conductive backing layer is a separate testable module. The electrical resistance from top to bottom along the trace is less than 1 Ω The leadframe acts as an acoustic antiwaveguide and does not channel the backward propagating acoustic waves [12], to enhance the reflection off of the rear surface.

The final 2D array is fabricated by thin line bonding the matching layer and piezoelectric layer onto the machined backing layer [13]. The backing layer is then diced into a pattern for the mating interconnect system, discussed below. The array is diced through the matching layer, the piezoelectric layer and partially into the backing layer. Dicing into the backing layer reduces the nearest neighbor acoustic cross talk. A schematic side cross sectional view of the diced array is shown in Figure 4. The saw kerf is shown hatched, and the leadframe traces are shown in black. At each side are inactive guard elements as previously shown in Figure 1.

Once diced, the 50 μm saw kerf in the array is back filled with a mixture of hollow glass microspheres in an epoxy matrix [14]. The microspheres have diameters less than 40 μm, a median diameter of 12 μm, and are mixed 3 parts to 1 part epoxy, by weight. The relative dielectric constant is 1.28. The kerf filling is used to protect and stabilize the fragile elements, but the kerf filling also reduces the directivity function of the individual elements. This will be discussed in Section IV. To provide a moisture seal and an electrical ground plane, the array has a thin Au plated Mylar film stretched and bonded across the front of the elements.

## III. Pad Grid Array Interconnect

### *A. Concept*

For a densely sampled 2D array, a demountable interconnect is desirable because it allows for the interchange of both the interconnect and the array with a minimal amount of rework. Such a demountable, high density interconnect technology, referred to as a Pad Grid Array was discussed at the 1992 SPIE Conference [15]. The interconnect technology used here is a larger size and higher density version of the PGA discussed in [15]. The basic concept is to terminate the coaxial signal cables onto flex circuits and to attach the flex circuits to a ceramic plate with a 50 x 50 grid of holes that matches the layout of the 2D array, hence a Pad Grid Array (PGA). The PGA provides 250 x 250 μm pads on a 300 x 300 μm pitch in a 50 x 50 grid. Further details of the PGA fabrication and specifications will be published elsewhere [16].

Since both the 2D array and the PGA are rigid bodies, a elastomeric member is required to provide mechanical compliance in order to achieve reliable connection between the 2D array and the PGA. An anisotropic elastomer, comprised of a silicone sheet 300 - 500 μm thick with 30 μm diameter Au plated wires on a 100 x 100 μm pitch spacing is used to connect the array and PGA together [17]. The anisotropic elastomer is shown schematically in Figure 5, both in cross section in a), and in a top view in b). The conductive wires protrude approximately 30 μm beyond both surfaces of the elastomer. The flush pads of the PGA and the approximately 10 μm high pads on the rear of the 2D array backing do not present any detectable arcing problems to adjacent elements at the typical excitation voltages of approximately 150 V. This elastomer requires approximately 300 psi to provide reliable electrical contact resistance of a few hundred mΩ This is an acceptable level given the high electrical

impedance of the individual array elements. The 100 μm spatial pitch of the wires in the elastomer was chosen to minimize registration requirements between the elastomer and both the array and the PGA. In the typical case, between 6 and 9 wires in the elastomer contact each pad. This connection can be confirmed by observing the footprint of the wires on the electrode pad on the rear of the 2D array backing material.

### *B. Partial PGA Assemblies*

Two partially terminated PGAs were fabricated in order to evaluate the interconnect technology. In each case, the PGA was fully assembled with a full set of flex circuits, but only a subset of the flex circuits were connected to the coaxial cables. A set of subarrays were terminated to evaluate regional uniformity. This pattern consisted of a central 8 x 8 subarray and 4 subarrays of 4 x 4 elements at the periphery. The total number of terminated elements was 128, and these were connected into a 128 channel cable assembly and connector. In the second partially terminated PGA, a "+" and an "x" pattern were chosen to evaluate linear uniformity across the whole array. The total number of terminated elements was 200, and these were connected into 2 separate 100 channel cable assemblies and connectors. Results from these partially terminated PGAs will be discussed in the next Section.

## IV. Measurement Results

### *A. Electrical Impedance*

To initially characterize the completed array, the electrical impedance was measured using an HP 4195 Impedance Analyzer. The test setup is shown schematically in Figure 6. A coaxial, 50 Ω tungsten tipped probe [18] was used to contact the array from the rear of the backing, while the return ground path was provided by the array ground foil and a grounding strip up to the coaxial probe. This method allows the array to be characterized independently of the interconnect. The impedance analyzer is calibrated and compensated for the length of the 50 Ω coaxial cable and the tungsten tip.

A typical plot of the magnitude of the electrical impedance is shown in Figure 7. The second notch in the impedance magnitude, where much of the power is transmitted, is 5.5 kΩ at 3.0 MHz. A characteristic plot of the real and the imaginary part of the electrical impedance is shown in Figure 8. The two peaks in the plot of Re{Z} are at 2.2 and 3.4 MHz. At the design center frequency of 2.5 MHz, Re{Z} = 4 kΩ and Im{Z} = -10 kΩ Clearly the impedance is dominated by the reactive component, due to the small capacitance of the element. Thus it is clear that such an element in a 2D array is not well matched to a typical 50 or 75 Ω cable. On transmit, the effect of the low efficiency from the mismatch may be partially compensated by the excitation pulse level, however, on receive, the small capacitance of the array element makes it inefficient to drive a typical 50 Ω cable. This observation is consistent with the concept of using multilayer ceramics to improve the electrical impedance matching [7]. An alternative is to include local circuitry such as impedance transformers or preamplifiers for each of the array elements [19], [20], [21]. For an array with many elements, an integrated approach to providing these electrical circuitry elements will be required.

### *B. Pulse Echo*

The 2D array module was first characterized by recording the pulse echo signals off of an immersed metal target. The array was probed with a coaxial tungsten wire tipped probe on the back of the array, as shown in Figure 6. The array was excited by a a 5052UA Panametrics pulser/receiver, and the return signal was analyzed with a digital scope. Measurements were made on one central row and one central column (100 total elements). The standard deviation in the peak-to-peak RF signal from element-to-element was +/- 50%. This variation exceeds that of commercial 1D phased arrays that are typically at least 50 times as large in area. Both variation in the material properties of the PZT and variations in the assembly techniques can contribute to this variation.

As a measure of the variation in the material properties of the PZT, both $k_t$ and the magnitude of the electrical impedance at the parallel resonance, $|Z(F_p)|$, were measured across a row of the PZT elements as air loaded resonators. The standard deviation in these quantities was +/- 10% and +/- 25%, respectively. Thus most of the variation in the pulse echo amplitudes appears to be accounted for by the PZT material variations. The remainder is due to variations in the other materials and in the assembly process. Variations in material properties of PZT of 15-20% are common for the dimensions used in 1D phased arrays. For the PZT material used in the array, the grain size is about 2.5 μm [22], thus the effects of variation due to grain boundaries is still averaged out at these small element dimensions. In actual use, 2D array elements are excited in groups, and this lowers the variation to levels more typical of 1D phased arrays.

To characterize the thermal stability of the array, and particularly the Z-axis backing with embedded BeCu wires, the array was thermally cycled for 24 hours at 50 C, 60 C, and 70 C. After each 24 hour thermal cycle, a representative set of pulse echo signals from one central row and one central column were measured with a coaxial tungsten wire tipped probe once the array had cooled back to room temperature.

The average pulse echo peak-to-peak signal magnitude dropped by 6% after the final 70 C cycle. The standard deviation in the peak-to-peak signal increased to +/- 58% after the final 70 C cycle. No loss of contact from the backing to any of the array elements was measured.

The 2D array and the PGA interconnect were evaluated as a system in a pulse echo mode as shown schematically in Figure 9. A computer (PC) is used to control a pulse generator for the system timing, a 128:1 MUX to select channels, and a digital scope to record the waveforms, through a IEEE-488 bus. The pulse generator triggers a 5052UA Panametrics pulser/receiver, and then the excitation pulse is routed to the desired channel through the MUX and onto the cable to the PGA. The array element is excited and the echo off a water immersed metal target is returned and stored in the digital scope. After a set of elements is interrogated the digital scope is instructed through the IEEE-488 bus to unload the digital scope memory into the PC for further analysis.

A typical pulse echo waveform from the array reflected off of a flat stainless steel target, 1.5 cm away, is shown in Figure 10. The near field / far field transition distance for a 250 μm element at 2.5 MHz is about 30 μm. Thus, the target is well into the far field. The total receiver gain for this waveform data is +20 dB, with an excitation voltage of 150 V from the pulser/receiver. The spectrum of this signal is shown in Figure 11, where the -6 dB center frequency of the spectrum is at 2.3 MHz, and the -6 dB fractional bandwidth is 50%. For this measurement, no additional series or shunt tuning elements were used in addition to the tuning provided by the approximately 3 meters of coaxial cable, with a characteristic impedance of 50 Ω

## *C. Directivity*

Although the kerf-fill material increases the mechanical robustness of the individual array elements, this comes at a cost of increased cross talk and reduced directivity of the element. A comparison of the single element directivity of air filled kerfs and epoxy/microsphere filled kerfs is shown in Figure 12. The -3dB value for the air filled kerf is 10 degrees, while the corresponding value for the filled kerf is 5 degrees. Clearly the kerf filling reduces the directivity of the elements.

## *D. Cross Talk*

The element-to-element cross talk determines the ability of an acoustic 2D array to adequately steer and to focus. For a 2D array, relevant cross talk comes from both electrical and acoustic sources. For this characterization a 200 V excitation pulse, from a 5052UA Panametrics pulser/receiver was applied through a 50 Ω tungsten tipped coaxial probe to the rear surface of the backing of an air loaded array, and the detected voltages were measured on the 9 nearest elements along a row through a second 50 Ω tungsten tipped coaxial probe, a 50 Ω cable, and a digital oscilloscope with a 50 Ω input impedance. This is a measurement of the electrical cross talk in the array and backing.

The data from this experiment is shown in Figure 13, where several components of the electrical cross talk are illustrated. The bottom curve, with the triangles, is the measurement system noise floor, showing the detected cross talk between the probes alone. The second lowest curve with the circles is the full array with a ground plane. The measurement of the array cross talk is compensated for the variation in the element sensitivity. The nearest neighbor cross talk is seen to be -42 dB, down from a 0 dB reference at the excited element. The voltage developed on the adjacent elements drops until about the 6th element where it levels off to about -70 dB. The curve with the squares is the array without a ground plane, i.e., floating acoustic elements. The top curve is the backing alone without a PZT layer.

Thus, most of the electrical cross talk is from the backing where there are 50 x 50 μm BeCu wires that are 250 μm apart for a 15 mm length, embedded in an epoxy matrix. When the array is grounded through the ground foil some of the signal is shunted through the piezoelectric elements to ground and this reduces the apparent cross talk on distant elements.

The PGA interconnect system has an electrical cross talk level of -60 dB in the frequency range of interest, and this is mostly determined by the flex circuit geometry [16]. The 500 μm thick elastomer, with 100 x 100 μm pitch wires, also has a measured electrical cross talk level of below -60 dB in the frequency range of interest.

## *E. Interconnect Uniformity*

In addition to the pulse height variation due directly to the 2D array, the elastomeric member also contributes to this variation. The effect of the elastomer was studied by examining the dependence of the pulse height variation on elastomer thickness, compression and spatial pitch. Three types of elastomers were investigated, 100 x 100 μm pitch of 300 μm thickness, 50 x 200 μm pitch of 300 μm thickness, and 100 x 100 μm pitch of 500 μm thickness. For these geometries, the 500 μm sample, with 35% compression, gave the best performance. With this elastomer, the elements had pulse echo waveforms that were characteristic of the 2D array transducer element variations. A random pattern of 3% of the total elements was not successfully connected by the elastomer, and varied with each reassembly of the array and PGA. The vari-

ations in pulse height, due to the elastomer, were also random with regard to position in the array or assembly history.

## V. DISCUSSION

In conclusion, a fully λ/2 sampled, 2.5 MHz, 2500 element 2D phased array was built and the initial single element performance was characterized both as an independent module, and through a demountable high density interconnect. Measurements were made on the electrical impedance, directivity and cross talk of the 2D array elements, as well as the pulse echo properties of the 2D array elements through the PGA interconnect. This work demonstrates the feasibility of the design and fabrication of such densely sampled 2D arrays. Further work, such as synthetic aperture reconstruction, is required to fully characterize the full 2D array performance.

## VI. ACKNOWLEDGMENTS

The authors gratefully acknowledge useful discussions with Martha Wilson, Raj Gururaja, and Pete Melton, and the generous help of King-Wah Yeung in the data acquisition and Ed Verdonk in the data analysis, of Hewlett-Packard, and the assistance of Bob Stanton, Paul Wheatcraft, Larry Daane, Michael Demeter, and Dan DeLessert of Precision Interconnect.

## VII. References

[1] D. H. Turnbull and F. S. Foster, "*Beam Steering with Pulsed Two-Dimensional Transducer Arrays*", IEEE Trans. on Ultrasonics, Ferroelectrics, and Frequency Control, Vol 38, 320-333 (Jul 1991).

[2] D. H. Turnbull and F. S. Foster, "*Simulation of B-Scan Images from Two-Dimensional Transducer Arrays: Part II - Comparison Between Linear and Two Dimensional Phased Arrays*", Ultrasonic Imaging, 344-353 (1992).

[3] S.W. Smith, G.E. Trahey and O.T. von Ramm, "*High Speed Ultrasound Volumetric Imaging System - Part I: Transducer Design and Beam Steering*", IEEE Trans. on Ultrasonics, Ferroelectrics, and Frequency Control, Vol 38, 100-115 (Jul 1991).

[4] S. W. Flax and M. O'Donnell, "*Phase Aberration Correction Using Signals From Point Reflectors and Diffuse Scatters: Basic Principles*", IEEE Trans. Ultrason., Ferroelec., Freq., Contr., Vol 35, 758-767, (1988).

[5] S.W. Smith, G.E. Trahey and O.T. von Ramm, "*Two Dimensional Arrays for Medical Ultrasound*", Proc. IEEE Ultrasonics Symposium, Vol 1, 625-628 (Nov 1991).

[6] S.W. Smith, G.E. Trahey and O.T. von Ramm, "*Two Dimensional Arrays for Medical Ultrasound*", Ultrasonic Imaging, Vol 14, 213-233 (1991).

[7] R.L. Goldberg, S.W. Smith, R.A. Ladew, and J.C.Brent, "*Multilayer PZT Transducer Arrays for Improved Sensitivity*", Proc. IEEE Ultrasonics Symposium, Vol 1, 551-554 (Nov 1992).
IEEE Ultrasonics Symposium, Vol 1, 625-628 (Nov 1991)

[8] D. H. Turnbull et al., "*Simulation of B-Scan Images from Two-Dimensional Transducer Arrays: Part I - Methods and Quantitative Contrast Measurements*", Ultrasonic Imaging, 323-343, (1992).

[9] Motorola Corporation, part number 3203HD.

[10] POCO Graphite DPF-3.

[11] M. G. Grewe and T. R. Gururaja, "Acoustic Properties of Particle/Polymer Composites for Transducer Backing Applications", IEEE Ultrasonics Symposium, Vol 2, 713-716 (Nov 1989).

[12] D. G. Miller and J. D. Larson III, US Patent 5,267,221, (Nov 1993).

[13] Bacon Industries.

[14] Eccospheres SDT-40, from Emerson Cummings, Canton, MA.

[15] S. Corbett and B. Stanton, "Conceptual Monolithic Pad Grid Array Connector for Transducer Interconnects", SPIE Vol 1733, 249-259 (Jul 1992).

[16] A discussion of the construction and performance details of the PGA will be published elsewhere.

[17] GB-Matrix Material, Shin Etsu Polymer America, Union City, CA.

[18] Ruckers and Kolls, San Jose, CA, part # 14860-001.

[19] H. Harada, US Patent, 4,926,380, (May 1990).

[20] M. G. Maginness, J. D. Meindl, and J. D. Plummer, US Patent 3,979, 711, (Sep. 1976).

[21] M. Greenstein, US Patent 5,329,498, (Jul. 1994).

[22] F. S. Foster, L. K. Ryan, and D. H. Turnbull, "*Characterization of Lead Zirconate Titanate Ceramics for Use in Miniature High-Frequency (20-80 MHz) Transducers*", IEEE Trans. on Ultrasonics, Ferroelectrics, and Frequency Control, Vol 38, 446-453 (Sep 1991).

## VIII. Figure Captions

Figure 1: Top view of one corner of the array, drawn to scale. The outside guard elements are shown hatched, the active elements each have a BeCu wire in the center.
Figure 2: Leadframe patterns. a) the trace leadframe, b) the spacer leadframe.
Figure 3: Cross-sectional view of the backing before machining to final dimensions. The dotted line represents the final dimension.
Figure 4: Side sectional view of the array, showing the matching layer, the piezoelectric layer, the diced kerf (hatched), and the embedded wires (black).
Figure 5: Anisotropic elastomer, a) cross sectional view of showing the protruding wires, b) top view to scale.
Figure 6: Schematic view of the test setup for the impedance measurements.
Figure 7: Magnitude of the electrical impedance for an element.
Figure 8: Real and imaginary parts of the electrical impedance for an element.
Figure 9: Schematic view of the test setup for the pulse echo measurements.
Figure 10: Waveform from 2D array through the PGA and cable.
Figure 11: Frequency spectrum from 2D array through the PGA and cable.
Figure 12: Directivity data for filled and unfilled kerfs.
Figure 13: Cross talk for an air loaded array.
Figure 14:

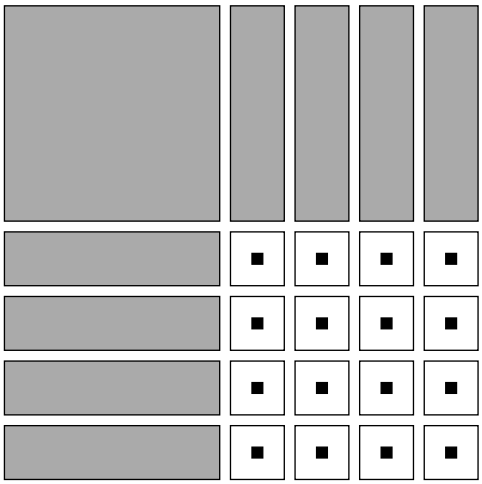

Figure 1:



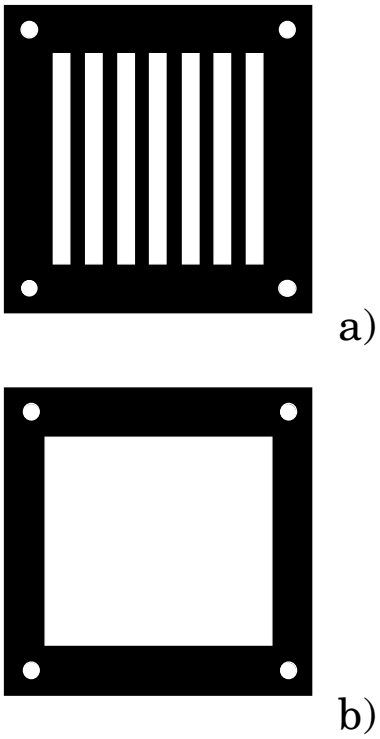


Figure 2:



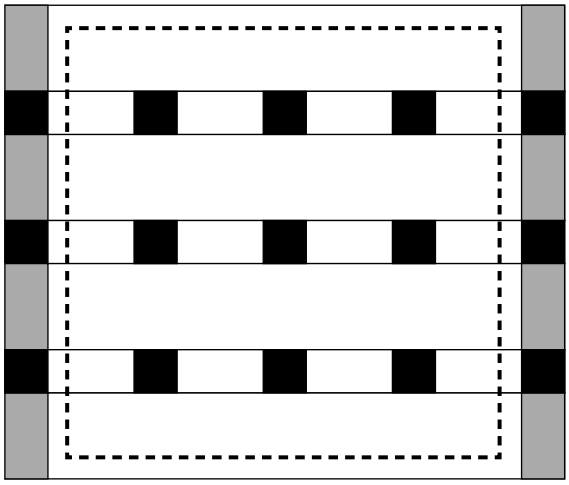

Figure 3:



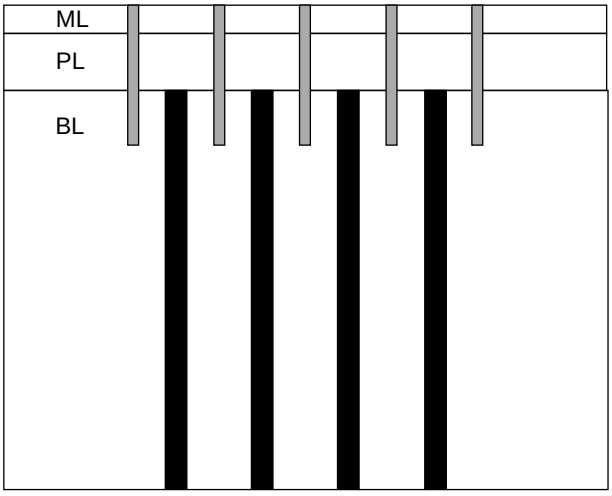


Figure 4:

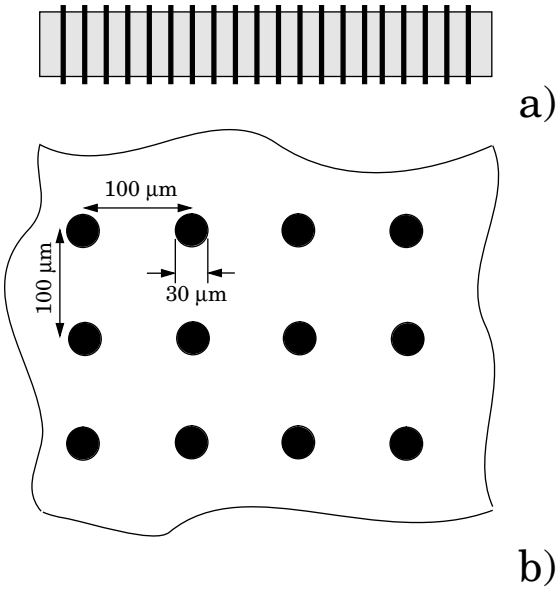


Figure 5:



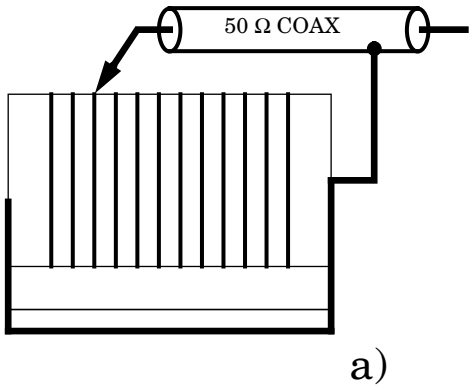


Figure 6:



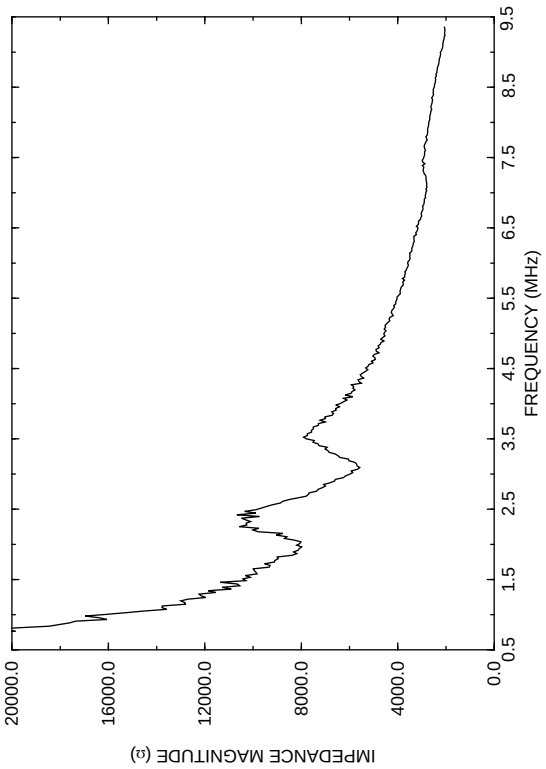


Figure 7:



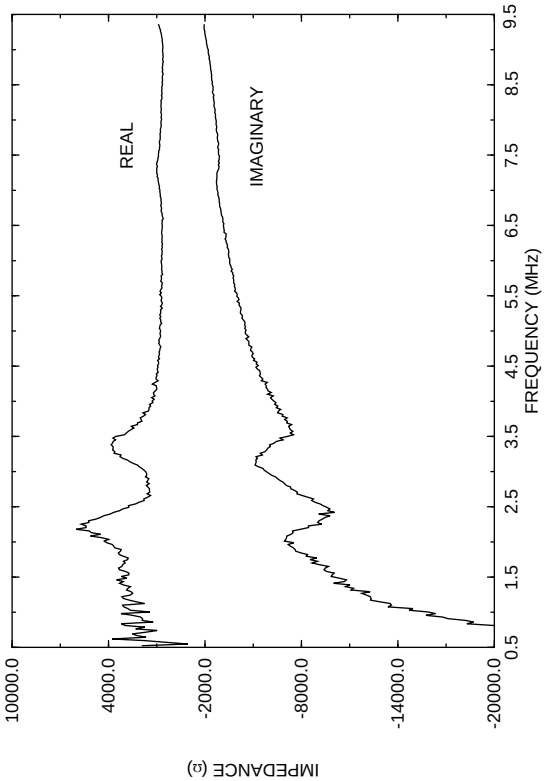


Figure 8:

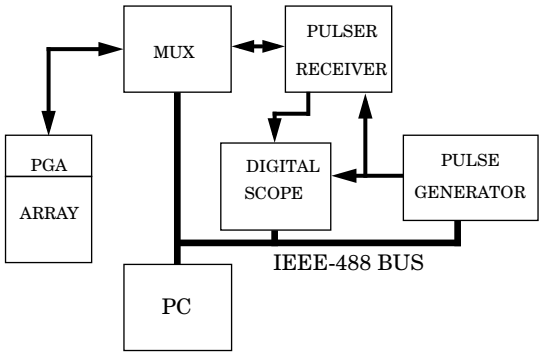


Figure 9:



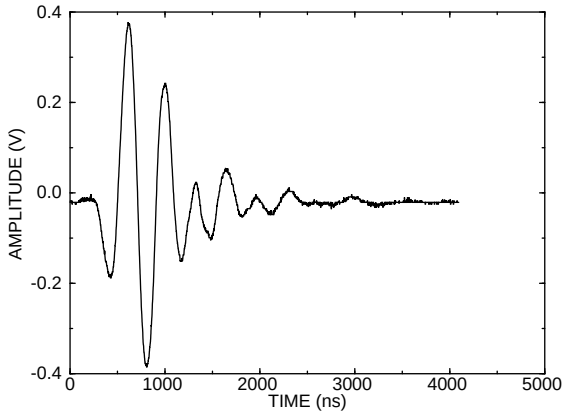


Figure 10:



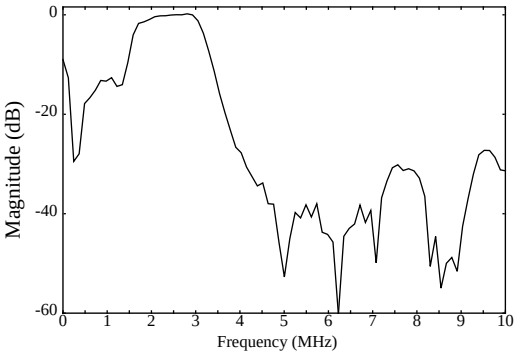


Figure 11:



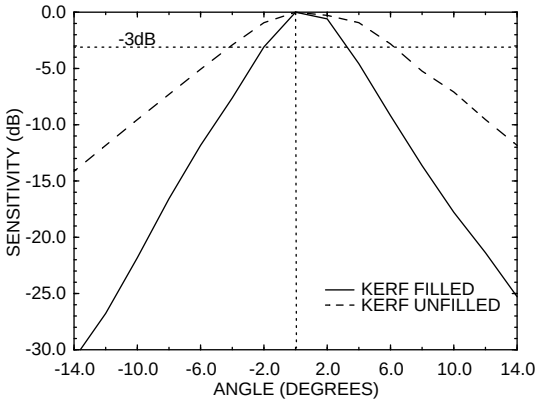


Figure 12: